Méditerranée
Revue géographique des pays méditerranéens
Journal of Mediterranean Geography

Search

INDEX
- Authors
- Keywords
- Geographical index

PRESENTATION
- The Journal
- Editorial Board
- Scientific Board
- Instructions for authors

FULL TEXT ISSUES
- 134 | 2022
  Public spaces and new urban compromises. Contrasted perspectives from the Mediterranean
- 133 | 2021
  Les paysages littoraux
- 132 | 2021
  The "Sustainable" City. Mediterranean Questions
- 131 | 2020
  Lebanon, a geography of contrasts
- 130 | 2018
  Portugal, a country in transformation
- 129 | 2017
  Portraying Mediterranean Cities
- 128 | 2017
  Evidence of climate change and its effects in the Mediterranean
- 127 | 2016
  Segregation in the cities of the European Mediterranean
- 126 | 2016
  Geomorphology and geoarchaeology of Black Sea coasts
- 125 | 2015
  Mediterranean coastal wetlands: dynamics and management issues
- 124 | 2015
  Changing spaces of economic activities in the Mediterranean basin
- 123 | 2014
  The quality of the environment in urban zones: a multidisciplinary assessment
- 122 | 2014
  Little Ice Age in Mediterranean
- 121 | 2013
  Great Wildfires in the Mediterranean
- 120 | 2013
  Agrarian aeras: landscape dynamics, ground laws, parties involved and planning
- 119 | 2012
  Water in the Eastern Mediterranean
- 118 | 2012
  Mediterranean rivers and their margins: processes and mangement
- 117 | 2011
  Geoarchaeology in the Mediterranean
- 116 | 2011
  North Africa and Globalization - Subalternity, territorial fragmentation
- 115 | 2010
  Mediterranean Coastline: withdraw towns back from the coastline; protect ourselves from the sea?
- 114 | 2010
  Cultural cities in the Mediterranean
- 113 | 2009
  Migrations and territories of mobility in the Mediterranean
- 112 | 2009
  La ricerca geoarcheologica in Italia
- 111 | 2008
  Port cities, Projections 2020: rising the stakes of development
- 110 | 2008
  Bulgaria-Romania: the new Balkan boundaries of the European Union
- 109 | 2007
  Terroirs : characterization, territorial developement and governance
- 108 | 2007
  Coastal hazards in the Mediterranean
- 107 | 2006
  New dynamics of rural development in the Southern Alps
- 106 | 2006
  Enterprises in Méditerranean: inheritances, models, redeployments
- 105 | 2005
  The great natural site in the metropolitan regions of Mediterranean
- 104 | 2005
  Coastal geoarchaeology of the Mediterranean

ALL ISSUES →

SECTIONS
- Paleoenvironment, Geoarchaeology, Historical Geography
- Environment, Landscape, Risk
- Ecosystems, Hydrology
- Rural Areas, Land Planning
- Economy, Innovation, Tourism
- Urban Spaces

CALL FOR PAPERS
- Call for papers – open
- Call for papers – closed

INFORMATION
- Contacts
- Crédits
- Publishing policies

FOLLOW US
- RSS feed

NEWSLETTERS
- OpenEdition Newsletter

OpenEdition Journals

Paleoenvironment, Geoarchaeology, Historical Geography

2023

Reconstruction of the Holocene Paleogeography of *Bani Salama*, *Wadi El-Natrun*, Egypt

Reconstitution de la paléogéographie holocène de Bani Salama, Wadi El-Natrun, *Égypte*

Gamal Younes, Clément Flaux, Isabelle Jouffroy-Bapicot and Nick Marriner

Abstracts

ENGLISH | FRANÇAIS

Wadi El-Natrun depression lies about 100 km north-west of Cairo, just south of the 'desert road' between Cairo and Alexandria. The depression has a longitudinal morphology extending from the southeast to the northwest with average dimensions of about 60 km × 15 km. *Bani Salama* site lies in the eastern part of the depression, to the east of *Fasda* Lake, which is located at -27 m below sea level. Based on a geomorphological survey and local archaeology, we found that the site has been occupied by human societies since at least around 4000 years before the present. The site contains ruins of a temple and a castle dating back to the 12th Dynasty of the Pharaonic period (1985-1773 BC). The site also contains workshops of raw glass production dating back to Egypt's Roman period (31 BC – AD 395). The aim of this study is to investigate the Holocene marsh deposits of *Bani Salama*, which are located between the Pliocene plateau and *Fasda* Lake. A sediment core (NAT-11) was taken from the site in June 2015. This core is investigated to understand the Holocene palaeo-geography, palaeoclimates and human impacts.

Outline

1. Introduction
2. Natural contexts of *Bani Salama*
3. Historical and archaeological background
4. Materials and methods
  4.1. GIS Design
  4.2. Core and radiocarbon dating
  4.3. Samples and analytical techniques
5. Results
  Unit A
  Unit B
  Unit C
  Unit D
6. Discussion
  Unit A
  Unit B
  Unit C
  Unit D
7. Palaeo-environmental reconstruction of *Bani Salama* site
8. Conclusions

Full text

*This research was supported by the Excellence Initiative of Aix-Marseille University (A*MIDEX, a French "Investissements d'Avenir" program) and the ANR project GEOMAR. We would also like to thank Mme Doriane Delanghe, Director of the Sedimentary Laboratory in CEREGE, Aix-Marseille University, for her support during the analysis of the sediment samples for this study.*

1. Introduction

1 *Bani Salama* lies in the eastern part of *Wadi El-Natrun* depression. The site contains ruins of a temple and a castle dating back to the 12th Dynasty (1985-1773 BC) (Fakhry, 1942; Callender, 2000). The site also contains some raw glass workshops dating back to Egypt's Roman period (31 BC - AD 395) (Nenna, 2010) (Fig. 1). The geomorphological and geological contexts of Beni Salama show the existence of a plateau on the eastern side, comprising Pliocene rocks. This plateau rises about 10 m above the Holocene marsh deposits, which lies to the west of it. *Fasda* Lake lies on the western side of the site, at a level of -27 m below sea level. Both the Pharaonic site and the Roman glass workshops are located above the Pliocene plateau on the eastern side. It is possible that past human societies exploited a nearby source of water during their occupation of the site, such as the lake. At present, *Wadi El-Natrun* depression contains four aquifers and the water flows from these aquifers into the depression (Youssef, Gad, and Ali, 2012).

2 The aim of this study is to reconstruct the Holocene paleogeography of *Bani Salama* site in *Wadi El-Natrun* depression at the time of ancient human occupation. Here, we use multi-proxy analyses (sedimentology, micropalaeontology, palaeoecology) of a core taken from the site to probe its environmental evolution during the Holocene. It is worth noting that it is the first time this type of research has been undertaken in this region. This study also seeks to answer some the following questions: When was the lake formed? How did *Fasda* lake levels change over time? What attracted human societies to the site? How did the environment evolve through time?

Fig. 1

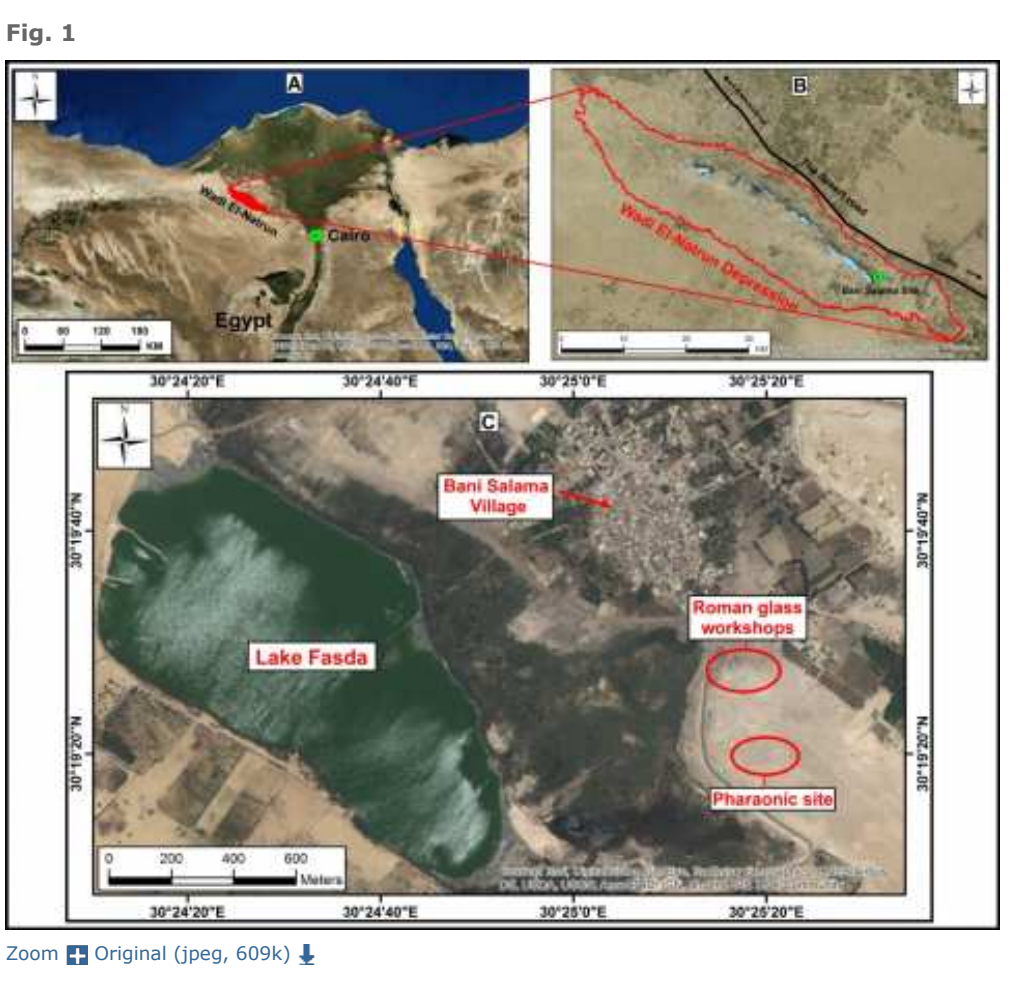

Zoom Original (jpeg, 609k)

(A) The general location of the study area. (B) The site of *Bani Salama* in the *Wadi El-Natrun* depression. (C) Details of the *Bani Salama* site.

This figure was produced using ArcGIS 10.1 (ArcMap) using a base image with a resolution of 30 m, taken on 25th April 2012 by Esri, Digital Globe, GeoEye, Earthstar Geographic, CNES/Airbus DS USDA, USGS, AeroGRID, IGN, and the GIS User Community and a satellite image "Landsat-8" captured on 4th January 2015 with a spatial resolution of 30 m.

2. Natural contexts of *Bani Salama*

3 Fasda Lake is the most important geomorphological trait of the *Bani Salama* site, and it is located-27 m below present sea level. This means that it is located about 11 m higher than the lowest point in *Wadi El-Natrun* depression. A marsh borders the eastern and northern parts of the lake. The marsh area has a width of about 700 m in the east, and 200 m in the north. The marsh sediments are of Holocene age. By contrast, the southern and western sides of the lake are bordered by Holocene aeolian sands (Fig. 2).

Fig. 2. Natural context of *Bani Salama*

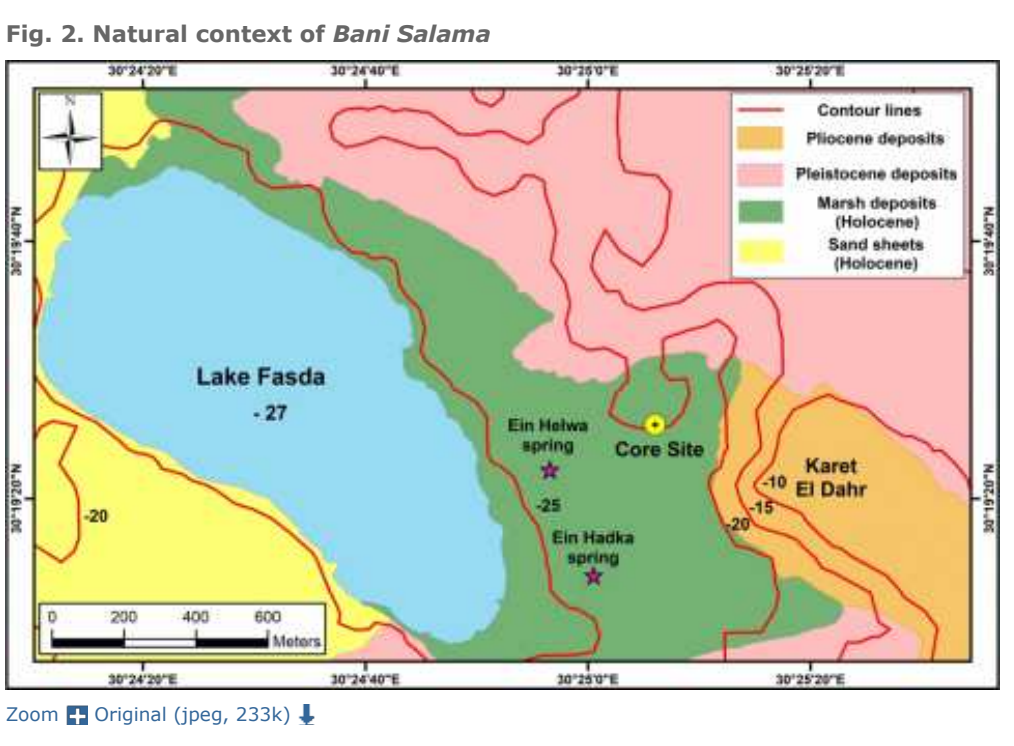

Zoom Original (jpeg, 233k)

This figure shows the geological, geomorphological and hydrological characteristics of the study area. It was drawn using a (Geological map 1987) produced by the Egyptian general petroleum corporation and CONOCO Coral Company, scale 1: 500,000. The digital elevation model (DEM) has a spatial resolution of 30 m and was produced using data from the Shuttle Radar Topography Mission (SRTM), NASA. The feature classes were drawn, and the contour lines were extracted from the DEM using ArcGIS 10.1.

4 To the east, directly above the marsh sediments lies a small plateau. It is about 10 m above the surrounding land. It is between 10 to 20 m below sea level. This small plateau is called "*Karet El Dahr*" (Fakhry, 1942). "*Karet El Dahr*" is part of the *Bani Salama* formation and is of Middle and Upper Pliocene age. The upper portion of this formation is dominated by an oyster bed, flinty limestone and argillaceous sands with a total thickness of about 30 m, while the lower portion is dominated by gypseous carbonaceous clay and sandy facies (Ahmed 1999). Pleistocene deposits comprise a grey calcareous sandstone layer with variable ratios of argillaceous material (Ahmed 1999). It flanks the site of *Bani Salama* from the north and south (Fig. 2).

5 *Wadi El-Natrun* depression contains four underground aquifers, groundwater being the most important source of water to replenish the lakes of the depression. The groundwater flows to the surface through springs because the levels of the springs and lakes are lower than that of the aquifers. Therefore, *Wadi El-Natrun* depression acts as a natural drainage basin for the aquifer system (Ahmed, 1999; Youssef, Gad, and Ali, 2012). Faults play an important role in the connections between the different aquifers and the water-saturated zones. The depth of the water table ranges between zero at the ground surface of *Wadi El-Natrun* lakes to 180 m to the west of *Wadi El-Natrun*. This means that *Wadi El-Natrun* depression acts like a sink area for these aquifers (Youssef, Gad, and Ali, 2012).

6 There are two springs to the east of *Fasda* lake at *Bani Salama*, where the groundwater flows through them to the surface and contributes to the lake's water supply. These springs are locally called "*Ein Hadka*", meaning "saline spring", in contrast to "*Ein Helwa*" meaning "freshwater spring" (Fig. 2) (Darwish, 1965).

7 Holocene deposits at *Bani Salama* can be divided into two units: marsh deposits to the east and north of *Fasda* Lake (fed by the outflowing aquifers) and aeolian sand deposits to the south and west (see Fig. 2). This unique geomorphology appears to have mediated the geography of past human occupation.

3. Historical and archaeological background

8 The "*Karet El Dahr*" site at *Bani Salama* is considered to be a past human settlement area, and it is divided into northern and southern parts. In the southern part lie the remains of a Pharaonic temple surrounded by a castle dating back to the 12th Dynasty (1985-1773 BC) (Callender, 2000), while in the northern part there are archaeological remains of workshops of raw-glass production dating back to the Roman period (Nenna, 2010). The remains of the outer walls of the Pharaonic fortress constitute mud bricks. A ditch encircles the walls for defensive purposes and inside the fortress granite blocks lie on the ground. An examination of them during our fieldwork revealed inscriptions and they can be attributed to the temple gate. The temple probably opened towards the east, and its other rooms and halls are still buried under the debris heaps lying to the west of the blocks (Fakhry, 1942). All the rocks at Wadi El-Natroun are sedimentary, so there is no presence of igneous rocks, including granite. In Egypt, granite only exists in the extreme south, in the east along the Red Sea coast and in South Sinai. Therefore, it is likely that the rocks used to build the gate of the Pharaonic temple were brought from outside the depression. The pink color of the granite used at *Bani Salama* suggests it was imported from Aswan, that located in southern Egypt on the banks of the Nile River.

9 The inscriptions and texts written on parts of the temple gate are difficult to decipher, and the threshold is broken into two halves. Nonetheless, the cartridges engraved on the blocks, the style of the hieroglyphics and the name of King "Amenemhat I" written in the middle of the threshold, show that the gate dates back to the reign of the first pharaohs of the 12th Dynasty. "Amenemhat I" ruled from 1985--1956 BC (Fakhry, 1942; Callender, 2000) (Fig. 3A).

10 A number of artifacts have been found during excavations of the site. These include part of a pyramid form, made of polished red granite and free of inscriptions. Also, a black granite bust with a hieroglyphic inscription on the back indicating that someone was honored by Ptah-Soker (Fakhry, 1942) (Fig. 3B). This black granite bust of a chancellor of the 18th Dynasty of Lower Egypt, and other remains at *Karet El Dahr*, imply that this region was held sacred around 2000 BC (Meinardus, 1992).

11 In the northern part of the "*Karet El Dahr*" another remnant of past human activites is the workshop "*Bani Salama*" for raw glass production dating back to the Roman period. Geophysical surveys were conducted at the *Bani Salama* workshop in 2000 and 2002. These surveys elucidated five buildings, and structures were identified as being furnaces for smelting and glass production. In 2003, excavation was conducted on several furnaces and glass smelters. This site was exceptional in view of the relatively large size of the furnaces and their excellent preservation in the archaeological record (Nenna *et al.*, 2005; Nenna, 2007) (Fig. 3C).

12 The *Bani Salama* workshop for raw glass production is located at the end of the tracks that formerly connected *Wadi El-Natrun* and *El-Tarrana* city, on the banks of the Rashid (or Rosetta) branch of the Nile River. El-Tarrana acted as a port for the export of raw glass to all parts of the Roman Empire (Nenna *et al.*, 2005). Based on the study by ((Nenna *et al.*, 2005), Fig. 4 was drawn from the (Topographic map, 1926) produced by the Egyptian Survey Authority, Scale 1:100000 called: "Wadi El Natrun". This map shows the ancient desert routes and tracks that connected the depression with *El-Tarrana*. This is further evidence for the historic importance of *Bani Salama* in raw glass production and its spatial relationships with the wider the Roman Empire.

Fig. 3.

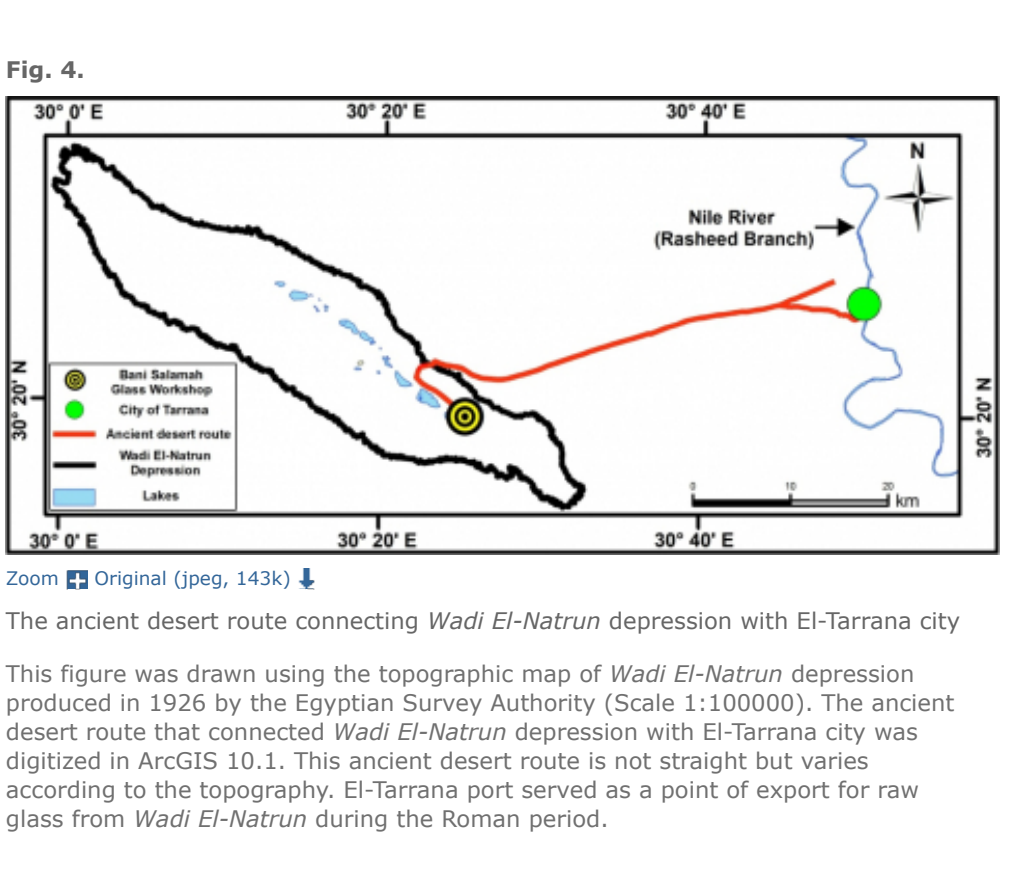

Zoom Original (jpeg, 621k)

(A) The blocks of the Pharaonic temple gate from the 12th Dynasty. (B) The black granite bust from the 18th Dynasty of the Pharaonic period. (C) Beni Salama workshop was used to produce raw glass during the Roman period.

The photos A & C were taken during field study in June 2015 by Clément Flaux. Photo B was taken from (Fakhry 1942) and is an artefact found at *Bani Salama*.

Fig. 4.

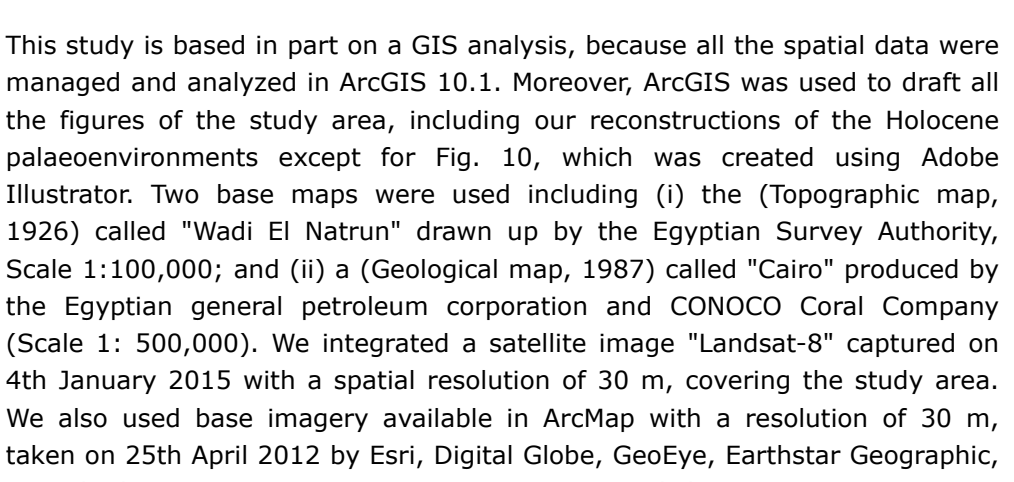
30° 0' E
30° 20' E
30° 40' E
30° 20' N
N
Nile River (Rasheed Branch)
Bani Salamah Glass Workshop
City of Tarrana
Ancient desert route
Wadi El-Natrun Depression
Lakes
km

Zoom Original (jpeg, 143k)

The ancient desert route connecting *Wadi El-Natrun* depression with El-Tarrana city

This figure was drawn using the topographic map of *Wadi El-Natrun* depression produced in 1926 by the Egyptian Survey Authority (Scale 1:100000). The ancient desert route that connected *Wadi El-Natrun* depression with El-Tarrana city was digitized in ArcGIS 10.1. This ancient desert route is not straight but varies according to the topography. El-Tarrana port served as a point of export for raw glass from *Wadi El-Natrun* during the Roman period.

4. Materials and methods

4.1. GIS Design

13 This study is based in part on a GIS analysis, because all the spatial data were managed and analyzed in ArcGIS 10.1. Moreover, ArcGIS was used to draft all the figures of the study area, including our reconstructions of the Holocene palaeoenvironments except for Fig. 10, which was created using Adobe Illustrator. Two base maps were used including (i) the (Topographic map, 1926) called "Wadi El Natrun" drawn up by the Egyptian Survey Authority, Scale 1:100,000; and (ii) a (Geological map, 1987) called "Cairo" produced by the Egyptian general petroleum corporation and CONOCO Coral Company (Scale 1: 500,000). We integrated a satellite image "Landsat-8" captured on 4th January 2015 with a spatial resolution of 30 m, covering the study area. We also used base imagery available in ArcMap with a resolution of 30 m, taken on 25th April 2012 by Esri, Digital Globe, GeoEye, Earthstar Geographic, CNES/Airbus DS USDA, USGS, AeroGRID, IGN, and the GIS User Community to draw all the phenomena. Our digital elevation model (DEM) has a spatial resolution of about 30 m. The feature classes were drawn using ArcGIS 10.1.

4.2. Core and radiocarbon dating

14 To study the palaeoenvironmental conditions and to reconstruct the Holocene palaeogeography of *Bani Salama*, we extracted a core (NAT-11) using a percussion corer in June 2015 (Fig. 5). Having georeferenced the maps, images and DEM data using ArcGIS 10.1, we studied the topography of the study area by defining contour lines and altimetric points. We subsequently chose the most suitable point to take the core, with an aim to extracting a long Holocene sediment archive (see Fig. 2). The length of this core is approximately 8 m. The purpose of this study is to investigate the environmental conditions that could have affected human activities in the past.

15 Radiocarbon dates were performed on eight peat samples at the Poznań Radiocarbon laboratory in Poland. The radiocarbon dates were calibrated using Calib 8.2 and the IntCal20 curve (Reimer et al. 2020). The bottommost sample was dated to 6899 - 6498 cal. BC and there were no inversions in the chronology. The radiocarbon ages are shown in Table 1 and Fig. 5.

4.3. Samples and analytical techniques

16 The core samples were analyzed at both the Chrono-Environment Laboratory in Besançon and the CEREGE Laboratory in Aix-en-Provence (France) in 2016. We analyzed the grain-size distributions on core samples to characterize the depositional environments (Marriner, Morhange, and Goiran, 2010; Delile *et al.*, 2015). Two different methods were used. The first method was wet sieving to separate the gravel (>2 mm), sand (2 mm – 63 µm) and silt and clay (<63 µm) fractions (Fig. 5). The second method was the dry sieving of five samples from unit A using a column of 15 sieves (Fig. 6). We also performed loss on ignition (LOI) of the core samples to characterize the moisture, organic matter and carbonate content of each unit. Samples were heated to temperatures of 105 °C (moisture), 550 °C (organic matter) and 950 °C (carbonate) respectively. Respective weights were calculated by subtracting weights before and after heating (Walter and Dean, 1974; Bengtsson and Enell, 1986; Heiri, Lotter, and Lemcke, 2001; Pansu and Gautheyrou, 2006). We also performed ostracod analysis of some core samples to probe past hydrological conditions. We obtained the ostracods from the sand fraction of the samples using a binocular microscope (Karanovic, 2012). Furthermore, we checked for pollen in 12 samples from unit D (See Fig. 8). Samples were prepared chemically (HCl, NaOH, HF, HCl, acetolysis) and physically (100 µm sieving) following the standard procedure of (Faegri, Kaland, and Krzywinski, 1989).

S	Sample name	Lab. no.	^{14}Cage BP	68.3% (1 sigma)	95.4% (2 sigma)	Agecal BC/AD
1	NAT11_35-40	Poz-88235	65 ± 30	Recent	Recent	-
2	NAT11_115-120	Poz-88236	300 ± 30	1521-1645 cal AD	1494-1656 cal AD	1562 cal AD
3	NAT11_155-160	Poz-88239	915 ± 30	1046-1199 cal AD	1038-121cal AD	1117 cal AD
4	NAT11_250-255	Poz-88240	1975 ± 30	8–110 cal AD	41 cal BC - 121 cal AD	44 cal AD
5	NAT11_375-378	Poz-88241	4400 ± 35	3089-2927 cal BC	3314-2910 cal BC	3017 cal BC
6	NAT11_450-455	Poz-88242	5620 ± 40	4493-4368 cal BC	4537-4359 cal BC	4445 cal BC
7	NAT11_580-585	Poz-88243	6930 ± 50	5877-5740 cal BC	5971-5722 cal BC	5810 cal BC
8	NAT11_605-615	Poz-88245	7820 ± 50	6741-6590 cal BC	6899-6498 cal BC	6648 cal BC

Table 1. ^{14}C dating of samples from the *Bani Salama* core

Analyses were performed by Poznań radiocarbon laboratory and the dates were calibrated using Calib 8.2 and the IntCal20 curve

Reimer *et al.*, 2020

5. Results

17 The core was taken from the marsh area to the west of "*Karet El Dahr*". It is located at the coordinates of latitude 30° 19' 28.02" N, and longitude 30° 25' 8.44" E, at -20 m below sea level (Fig. 2). In this section, we describe the stratigraphic units of the core, from bottom to top (Fig. 5).

Unit A

18 This unit is 6 to 8 m below the surface and is yellow in colour (Munsell code: 2.5 Y 6/4). Unit A does not contain organic materials, but we dated the bottom most sample of the overlying unit. According to the radiocarbon dates for this sample (Fig. 5 and Table 1), unit A was deposited before about 6648 cal. BC. We carried out wet sieving grain-size analyses for 8 samples from this unit. The average percentage of silt and clay is 19.2% while the average percentage of sand is 80.8% and there is no gravel. The sand fraction was subsequently dry sieved, and the results analyzed using the software GRADISTAT v. 9.1 developed by (Blott and Pye 2001) based on the grain-size parameters proposed by (Folk and Ward, 1957) (see Fig. 6). We found that these samples were dominated by medium sand with a mean (Mz) index of 1.832 Ø. Four of the samples were moderately sorted with an average sorting (σ) index of 0.894 Ø while one sample at 605-615 cm was poorly sorted with a sorting (σ) index of 1.040 Ø. The LOI results indicate that this unit has a moisture content of just 0.1%, organic matter content is 0.3% and carbonate content is 0.1% (See Fig. 5). There are no ostracods or organic material in this unit.

Fig. 5. The sediment core from *Bani Salama*

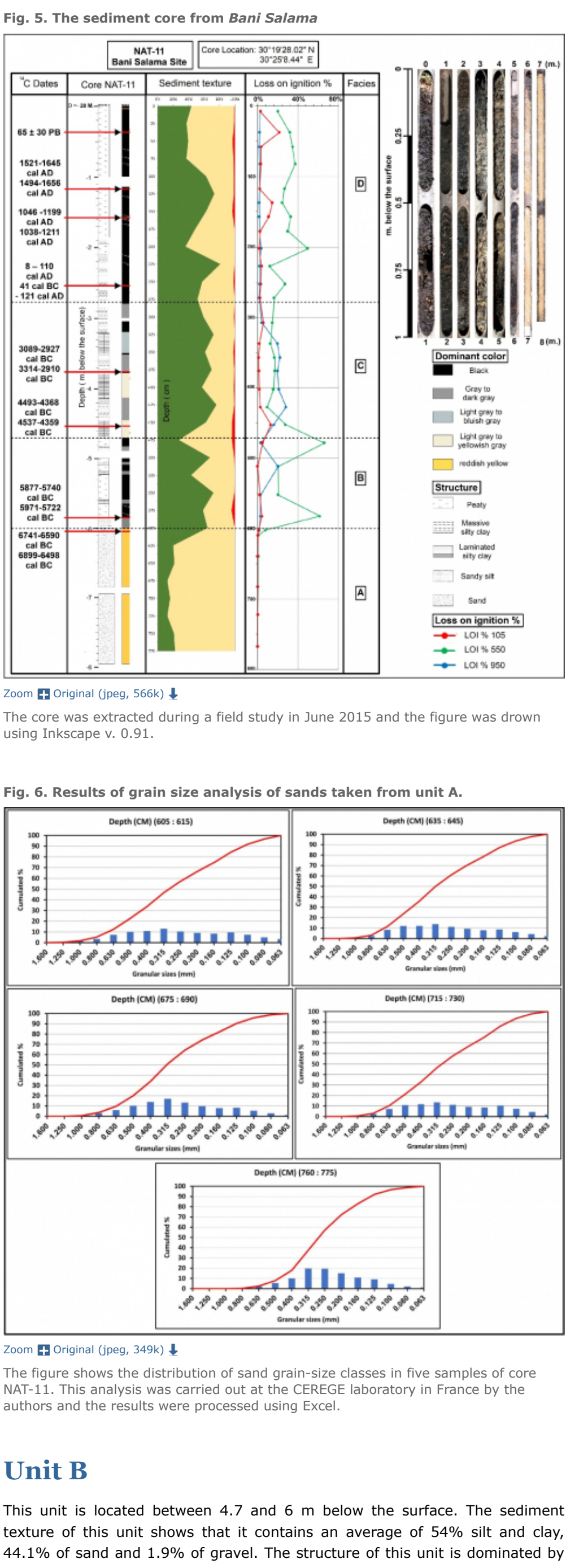

Zoom Original (jpeg, 566k)

The core was extracted during a field study in June 2015 and the figure was drawn using Inkscape v. 0.91.

Fig. 6. Results of grain size analysis of sands taken from unit A.

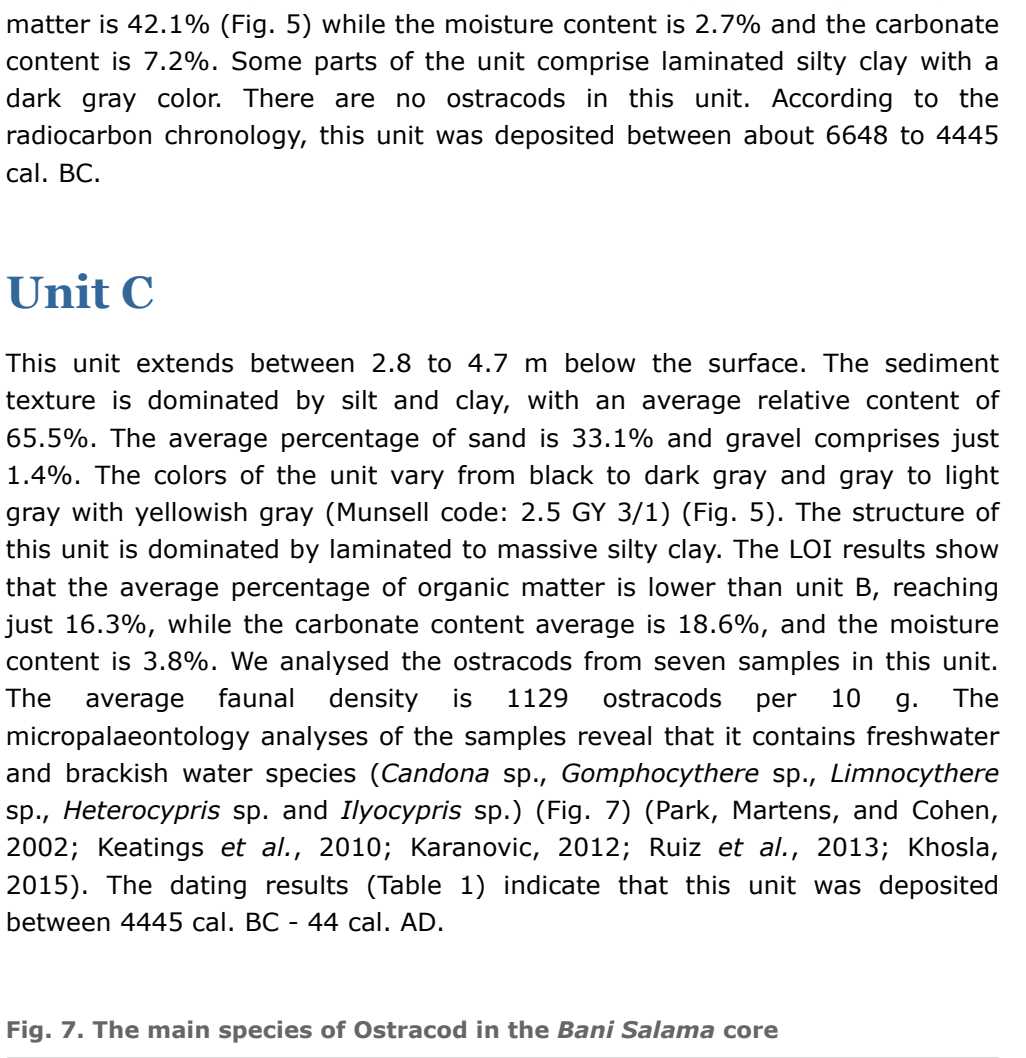

Zoom Original (jpeg, 349k)

The figure shows the distribution of sand grain-size classes in five samples of core NAT-11. This analysis was carried out at the CEREGE laboratory in France by the authors and the results were processed using Excel.

Unit B

19 This unit is located between 4.7 and 6 m below the surface. The sediment texture of this unit shows that it contains an average of 54% silt and clay, 44.1% of sand and 1.9% of gravel. The structure of this unit is dominated by peat and organic components and is black in color with Munsell code (N 1.5). This is confirmed by the LOI results, where the average percentage of organic matter is 42.1% (Fig. 5) while the moisture content is 2.7% and the carbonate content is 7.2%. Some parts of the unit comprise laminated silty clay with a dark gray color. There are no ostracods in this unit. According to the radiocarbon chronology, this unit was deposited between about 6648 to 4445 cal. BC.

Unit C

20 This unit extends between 2.8 to 4.7 m below the surface. The sediment texture is dominated by silt and clay, with an average relative content of 65.5%. The average percentage of sand is 33.1% and gravel comprises just 1.4%. The colors of the unit vary from black to dark gray and gray to light gray with yellowish gray (Munsell code: 2.5 GY 3/1) (Fig. 5). The structure of this unit is dominated by laminated to massive silty clay. The LOI results show that the average percentage of organic matter is lower than unit B, reaching just 16.3%, while the carbonate content average is 18.6%, and the moisture content is 3.8%. We analysed the ostracods from seven samples in this unit. The average faunal density is 1129 ostracods per 10 g. The micropalaeontology analyses of the samples reveal that it contains freshwater and brackish water species (*Candona* sp., *Gomphocythere* sp., *Limnocythere* sp., *Heterocypris* sp. and *Ilyocypris* sp.) (Fig. 7) (Park, Martens, and Cohen, 2002; Keatings *et al.*, 2010; Karanovic, 2012; Ruiz *et al.*, 2013; Khosla, 2015). The dating results (Table 1) indicate that this unit was deposited between 4445 cal. BC - 44 cal. AD.

Fig. 7. The main species of Ostracod in the *Bani Salama* core

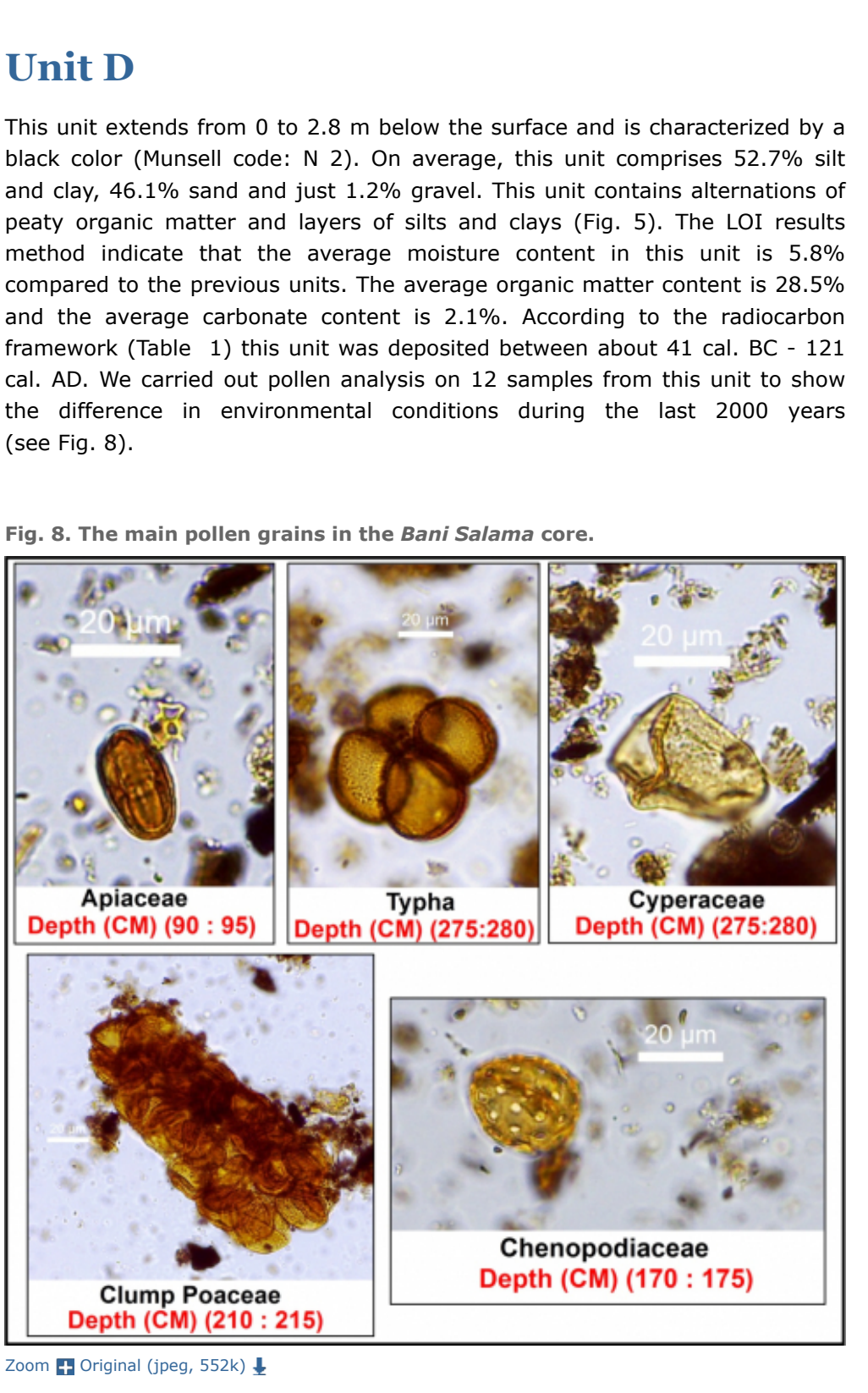

Zoom Original (jpeg, 369k)

Ostracod species include (*Candona* sp., *Gomphocythere* sp., *Limnocythere* sp., *Heterocypris* sp. and *Ilyocypris* sp.). This analysis was carried out by the authors at the Chrono-Environment Laboratory in Besançon, France.

Unit D

21 This unit extends from 0 to 2.8 m below the surface and is characterized by a black color (Munsell code: N 2). On average, this unit comprises 52.7% silt and clay, 46.1% sand and just 1.2% gravel. This unit contains alternations of peaty organic matter and layers of silts and clays (Fig. 5). The LOI results method indicate that the average moisture content in this unit is 5.8% compared to the previous units. The average organic matter content is 28.5% and the average carbonate content is 2.1%. According to the radiocarbon framework (Table 1) this unit was deposited between about 41 cal. BC - 121 cal. AD. We carried out pollen analysis on 12 samples from this unit to show the difference in environmental conditions during the last 2000 years (see Fig. 8).

Fig. 8. The main pollen grains in the *Bani Salama* core.

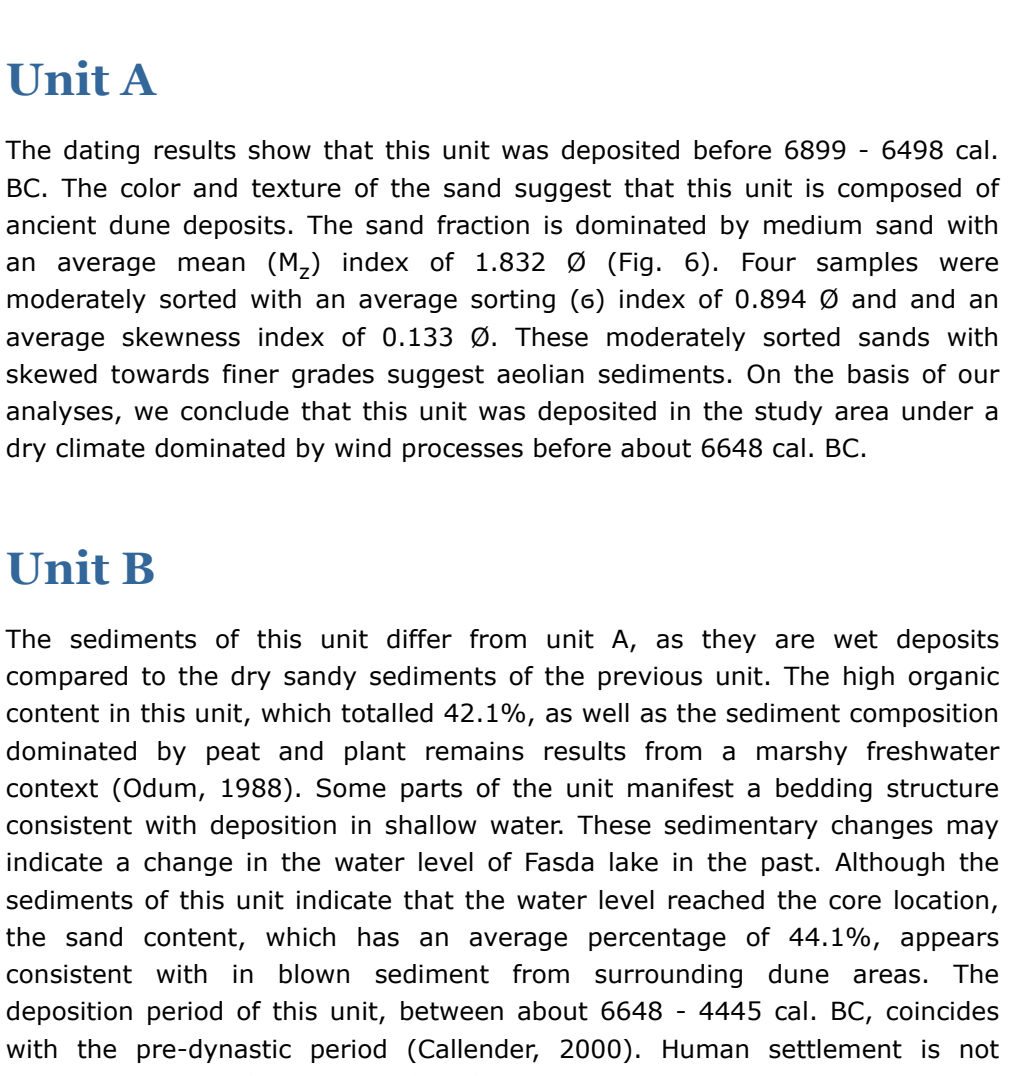

Zoom Original (jpeg, 552k)

The figure shows some pollen types from the *Bani Salama* core (Typha, Apiaceae, Chenopodiaceae, Cyperaceae and Poaceae). This analysis was carried out by the authors at the Chrono-Environment Laboratory in Besançon, France.

6. Discussion

22 According to the results reported above, we can interpret the Holocene marsh deposits of *Bani Salama*, which are located between the Pliocene plateau and *Fasda* lake, to understand the Holocene palaeogeography and human impacts in the area.

Unit A

23 The dating results show that this unit was deposited before 6899 - 6498 cal. BC. The color and texture of the sand suggest that this unit is composed of ancient dune deposits. The sand fraction is dominated by medium sand with an average mean (M_z) index of 1.832 Ø (Fig. 6). Four samples were moderately sorted with an average sorting (σ) index of 0.894 Ø and and an average skewness index of 0.133 Ø. These moderately sorted sands with skewed towards finer grades suggest aeolian sediments. On the basis of our analyses, we conclude that this unit was deposited in the study area under a dry climate dominated by wind processes before about 6648 cal. BC.

Unit B

24 The sediments of this unit differ from unit A, as they are wet deposits compared to the dry sandy sediments of the previous unit. The high organic content in this unit, which totalled 42.1%, as well as the sediment composition dominated by peat and plant remains results from a marshy freshwater context (Odum, 1988). Some parts of the unit manifest a bedding structure consistent with deposition in shallow water. These sedimentary changes may indicate a change in the water level of Fasda lake in the past. Although the sediments of this unit indicate that the water level reached the core location, the sand content, which has an average percentage of 44.1%, appears consistent with in blown sediment from surrounding dune areas. The deposition period of this unit, between about 6648 - 4445 cal. BC, coincides with the pre-dynastic period (Callender, 2000). Human settlement is not attested at *Bani Salama* during this phase.

Unit C

25 This unit consists of 65.5% laminated silt and clay with low organic matter content, deposited as thinly bedded layers and containing freshwater ostracods. This unit formed inside a shallow freshwater body with quiet-water conditions allowing deposition of fine-grained suspended sediment like silt, clay and sands (Boggs, 2006). This also suggests that *Fasda* Lake was much larger at this time and spread east to the level of NAT-11 core (Fig. 2). According to the dating results for this unit, the existence of *Fasda* Lake and the formation of lacustrine sediments at the core site coincided with the human occupation of the *Bani Salama* site during the Pharaonic period (3200 - 332 BC), the Ptolemaic Period (332 - 31 BC) (Callender, 2000) and shortly before the beginning of the Roman period in Egypt (31 BC - AD 395) (Nenna, 2010). As the core data indicates, the level of *Fasda* Llake was about 4 m higher than at present. This higher freshwater lake level was particularly conducive to human activities.

Unit D

26 This unit began to be deposited between about 41 cal. BC – 121 cal. AD until the present time, meaning that it was deposited during the last ~2000 years. It includes the Roman occupation of *Bani Salama* (Nenna, 2010). The texture of this unit is very similar to unit B because it comprises successive layers of peat and silt and clay. This is consistent with past fluctuations in the level of *Fasda* Lake. The amount of organic content in this unit is less than in unit B, reaching only 28.5%. The palynological analyses of this unit reveal the presence of Typha, Apiaceae, Chenopodiaceae, Cyperaceae and Poaceae pollen (Fig. 8). During the field study of *Beni Salama*, we found that these plants are still growing in the area today. This suggests that the climatic and hydrological conditions of the area remained relatively stable in the study area during the deposition period of unit D.

7. Palaeo-environmental reconstruction of *Bani Salama* site

27 Data from the *Bani Salama* core (Figs. 5 and 6) demonstrate that the site was characterized by a dry environment dominated by aeolian processes until the first quarter of the Holocene period, before about 6899 - 6498 cal. BC. This may explain why *Bani Salama* was not occupied by human societies until this date, as attest historical and archaeological data (Fig. 9A). According to NAT-11 sediment core and the dating results, water entered the site of *Bani Salama* between 6648 - 5810 cal. BC via the groundwater that fed the springs and led to the formation of marsh areas. Marsh/lacustrine sediments began to form at the position of the core site as a result of increased groundwater flow to the site and the expansion of *Fasda* Lake. Figure 9B shows that the lake's water level between 3314 - 2910 cal BC was -23.80 m below sea level, about 3 m higher than the current situation. According to current archaeological findings, the emergence of human occupation at *Bani Salama* began during the 12th Dynasty (1985 - 1773 BC) when the Pharaonic castle and temple were built next to *Fasda* Lake, on top of *Karet El Dahr* (Fakhry, 1942; Callender, 2000). The results of the ostracod analysis (Fig. 7) show that *Fasda* Lake comprised freshwater, an important natural resource that attracted human societies to *Bani Salama* at this time. Figure 9C indicates that the level of the lake continued to rise to around -22.80 m below sea level, between 41 cal. BC – 121 cal. AD. At the same time, the lake's water receded from the position of the sediment core and the marsh began to form again around the fringes of the lake. During this period, *Bani Salama* workshop was founded to produce raw glass during Roman times in the northern part of *Karet El Dahr* (Nenna, 2010). The decision to establish a glassmaking workshop at *Bani Salama* during the Roman period is probably due to the availability of basic materials such as sand and natron salts that were in abundant supply around the lake. Indeed, *Bani Salama* was one of the most important glass production centers in the Roman Empire (Nenna, 2010). The raw glass blocks were transported from *Bani Salama* to the port of El-Tarrana, on the banks of the Nile, and were then loaded onto ships and exported overseas (Nenna *et al.*, 2005). Results of the pollen analysis (Fig. 8) indicate that we find the same plants today as 2000 years ago. The level of *Fasda* Lake has decreased by 4.2 m and dropped to -27 m below the sea level and its area has shrunk and been replaced by marsh deposits (see Fig. 9D). The shrinking of the lake is probably due to a fall in water supply from the springs, consistent with decreasing Nile flow and increased aridity. At *Fasda* Lake this transition is attested by a gradual transformation from fresh to saline water, due to the concentration of dissolved ions because the lake has no outlet. These relationships demonstrate that *Fasda* Lake has responded to a gradual precession-driven shift in the mean boreal position of the ITCZ (Fig. 10). A time-progressive decrease in summer insolation reduced Africa's land/sea contrast and therefore the northern movement of monsoonal rainfall belts, which, for the Nile valley, lay ~500 km north of present during the early Holocene (Marriner *et al.*, 2012). Convective activity within the ITCZ was furthermore reduced by a gradual decrease in monsoon wind strength over East Africa, and therefore moisture influx from the southern Indian Ocean (Bassinot *et al.*, 2011). Nonetheless, our results suggest that relatively high lake levels persisted at *Fasda* Lake beyond the end of the African Humid Period because the lake was fed by groundwater.

8. Conclusions

28 This study focused on the analysis of the Holocene deposits at *Bani Salama* with the aim of reconstructing the palaeoenvironments when human societies occupied the site. Before 6899 - 6498 cal BC, *Bani Salama* was characterized

by a dry climate dominated by aeolian processes. Water entered the site of *Bani Salama* between 6648 - 5810 cal BC via groundwater-fed springs, leading to the formation of *Fasda* Lake. Human occupation began at *Bani Salama* between 1985 - 1956 BC, when the Pharaonic castle and temple were built next to *Fasda* Lake, on top of *Karet El Dahr* during the 12th Dynasty. After the African Humid Period, societies were concentrated along the Nile Valley, desert oases and spring outlets such as Wadi Natroun. The results of the ostracod analysis indicate that *Fasda* Lake contained freshwater, making the site particularly attractive to human societies at that time. *Bani Salama* was one of the most important glass production centers during the Roman Empire and it was selected as a glassmaking site due to the availability of raw materials, such as sand and natron salts that were deposited around the lake. The raw glass blocks were transported from *Bani Salama* to El-Tarrana city and were there loaded onto ships and exported abroad through the Nile Rasheed branch and then across the Mediterranean to all parts of the Roman Empire. According to our core data, there were significant changes in the levels of *Fasda* Lake where the highest elevation of the lake was -22.80 m between 41 cal BC – 121 cal AD. At present, we find that the surface level of *Fasda* lake has dropped to -27 m. A reduction in the surface area of the lake is due to a fall in water supply from the groundwater-fed springs.

Fig. 9. Reconstruction of the Holocene paleogeography of *Bani Salama*

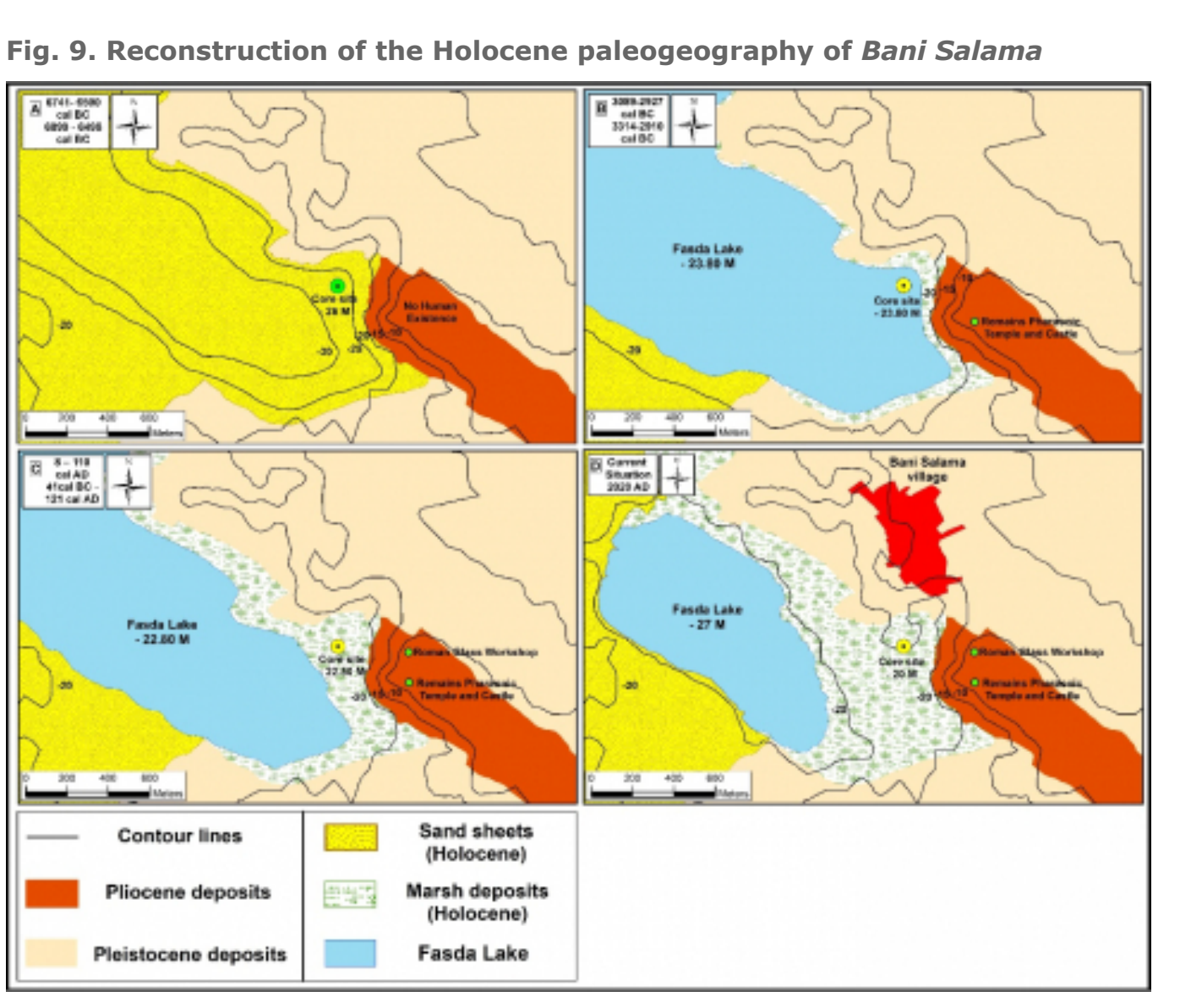

Zoom Original (jpeg, 566k)

This figure shows the evolving geomorphology of the study area during four different stages, from around 6600 cal. BC to the present

The maps were drawn using ArcGIS, based on the core data from our study, maps and the digital elevation model (DEM).

Fig. 10. Tentative reconstruction of *Fasda* Lake levels during the past 8000 years and comparison with other regional proxies

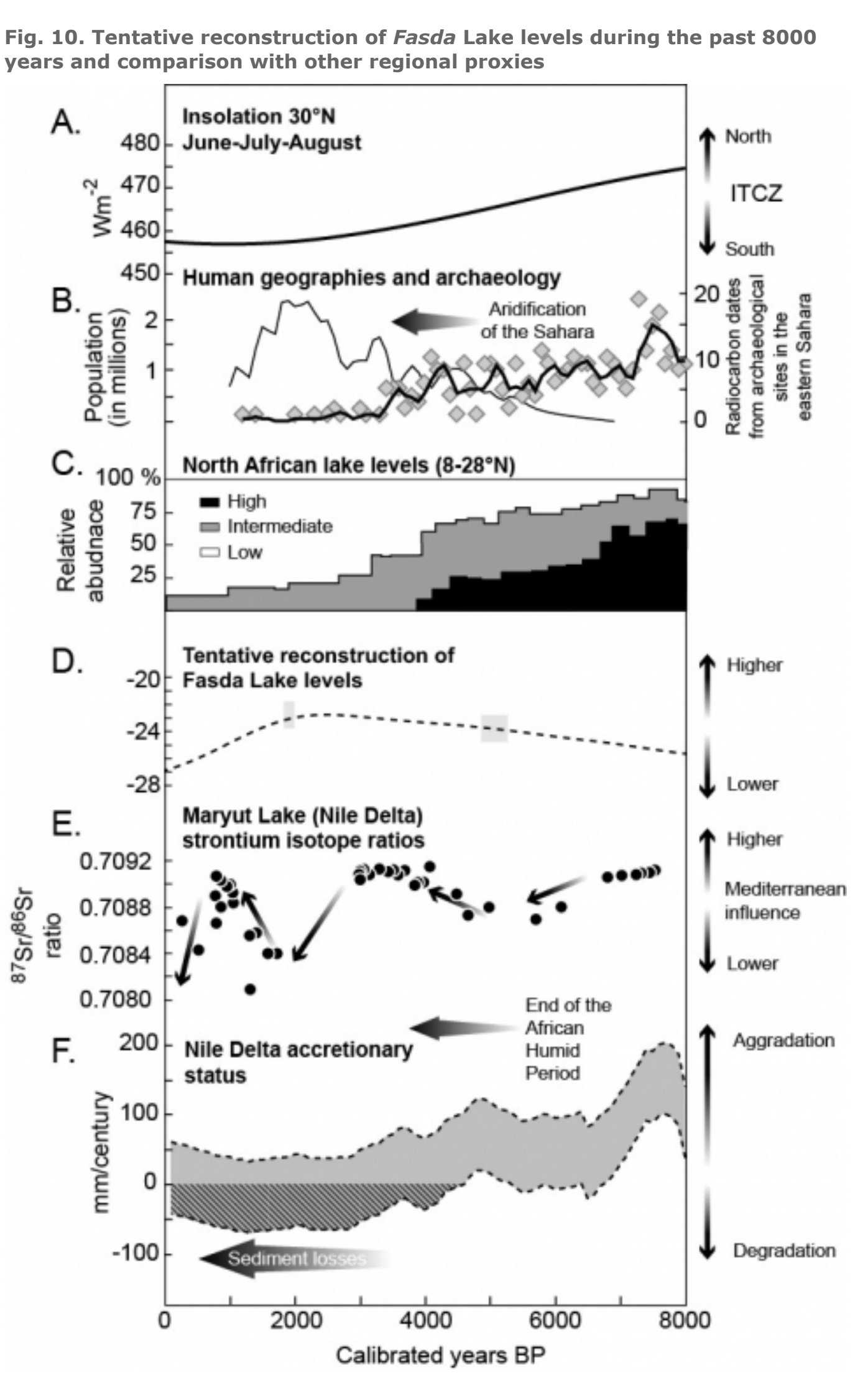

Zoom Original (jpeg, 165k)

Holocene insolation at 30°N for June-July-August (Laskar *et al.*, 2004). (B) On the right axis: radiocarbon dates from early and mid-Holocene occupation sites in the Eastern Sahara (Kuper and Kröpelin, 2006). The solid black line denotes a three-point moving average. On the left axis: estimates for the population of the Nile valley in Egypt (Butzer, 1976). (C) North African lake levels (Magny *et al.*, 2013). (D) Reconstruction of *Fasda* Lake levels from core Nat-11 (this study). (E) Strontium isotope record from Mayut Lake on the western margin of the Nile Delta showing variations in the influence of the Mediterranean Sea and Nile flow in the lake's palaeohydrology (Flaux *et al.*, 2013). (F) Nile Delta accretionary status (Marriner *et al.*, 2013).

This figure was created by Illustrator 25.2. 1 software.

29 Ahmed, S. A. 1999. *Hydrogeological and Isotope Assessment of Ground Water in Wadi El-Natrun and Sadat City Egypt*. Cairo: Faculty of Science, Ain Shams University, M. Sc. Thesis.

30 Bassinot, F. C., C. Marzin, P. Braconnot, O. Marti, E. Mathien-Blard, F. Lombard, and L. Bopp. 2011. Holocene evolution of summer winds and marine productivity in the tropical Indian Ocean in response to insolation forcing: data-model comparison. *Climate of the Past* 7 (3):815-829.

31 Bengtsson, L., and M. Enell. 1986. Chemical analysis. In *Handbook of Holocene Palaeoecology and Palaeohydrology*, ed. B. E. Berglund, 423-451. Chichester, UK: John Wiley & Sons Ldt.

32 Blott, S. J., and K. Pye. 2001. GRADISTAT: a grain size distribution and statistics package for the analysis of unconsolidated sediments. *Earth Surface Processes and Landforms* 26 (11):1237-1248.

33 Boggs, S. 2006. *Principles of sedimentology and stratigraphy* 4th ed. Upper Saddle River, New Jersey: Pearson Prentice Hall.

34 Butzer, K. W. 1976. *Early hydraulic civilization in Egypt: a study in cultural ecology*. Chicago London: The University of Chicago Press.

35 Callender, G. 2000. The Middle Kingdom Renaissance (c.2055-1650 BC). In *The Oxford History of Ancient Egypt*, ed. I. Shaw, 148-217. Oxford, UK: Oxford University Press.

36 Darwish, M. H. 1965. *Geology and mineralogy of saline deposits of wadi El-Natrun Egypt*. Cairo: Faculty of Science, Ain Shams University, M. Sc. Thesis.

37 Delile, H., A. Abichou, A. Gadhoum, J.-P. Goiran, E. Pleuger, J.-Y. Monchambert, A. Wilson, E. Fentress, J. Quinn, I. Ben Jerbania, and F. Ghozzi. 2015. The Geoarchaeology of Utica, Tunisia: The Paleogeography of the Mejerda Delta and Hypotheses Concerning the Location of the Ancient Harbor. *Geoarchaeology* 30 (4):291-306.

38 Faegri, K., P. E. Kaland, and K. Krzywinski. 1989. *Textbook of pollen analysis.* Chichester UK: John Wiley & Sons Ltd.

39 Fakhry, A. 1942. *Recent explorations in the oases of the western desert*. Press of the French Institute of Oriental Archaeology.

40 Flaux, C., C. Claude, N. Marriner, and C. Morhange. 2013. A 7500-year strontium isotope record from the northwestern Nile delta (Maryut lagoon, Egypt). *Quaternary Science Reviews* 78:22-33.

41 Folk, R. L., and W. C. Ward. 1957. Brazos River bar: a study in the significance of grain size parameters. *Journal of sedimentary research* 27 (1):3-26.

42 Geological map. 1987. Called "Cairo", Scale 1: 500,000. Map sheets NH36NW and NH35NE. Produced by CONOCO Coral Company with cooperation of the Egyptian General Petroleum Corporation, Cairo.

43 Heiri, O., A. F. Lotter, and G. Lemcke. 2001. Loss on ignition as a method for estimating organic and carbonate content in sediments: reproducibility and comparability of results. *Journal of Paleolimnology* 25 (1):101-110.

44 Karanovic, I. 2012. *Recent Freshwater Ostracods of the World: Crustacea, Ostracoda, Podocopida*. Berlin, Heidelberg: Springer.

45 Keatings, K., J. Holmes, R. Flower, D. Horne, J. E. Whittaker, and R. H. Abu-Zied. 2010. Ostracods and the Holocene palaeolimnology of Lake Qarun, with special reference to past human–environment interactions in the Faiyum (Egypt). *Hydrobiologia* 654 (1):155-176.

46 Khosla, A. 2015. Palaeoenvironmental, palaeoecological and palaeobiogeographical implications of mixed fresh water and brackish marine assemblages from the Cretaceous-Palaeogene Deccan intertrappean beds at Jhilmili, Chhindwara District, central India. *Revista Mexicana de Ciencias Geológicas* 32 (2):344-357.

47 Kuper, R., and S. Kröpelin. 2006. Climate-Controlled Holocene Occupation in the Sahara: Motor of Africa's Evolution. *Science* 313 (5788):803-807.

48 Laskar, J., P. Robutel, F. Joutel, M. Gastineau, A. C. M. Correia, and B. Levrard. 2004. A long-term numerical solution for the insolation quantities of the Earth. *Astronomy & Astrophysics* 428 (1):261-285.

49 Magny, M., N. Combourieu-Nebout, J. L. de Beaulieu, V. Bout-Roumazeilles, D. Colombaroli, S. Desprat, A. Francke, S. Joannin, E. Ortu, O. Peyron, M. Revel, L. Sadori, G. Siani, M. A. Sicre, S. Samartin, A. Simonneau, W. Tinner, B. Vannière, B. Wagner, G. Zanchetta, F. Anselmetti, E. Brugiapaglia, E. Chapron, M. Debret, M. Desmet, J. Didier, L. Essallami, D. Galop, A. Gilli, J. N. Haas, N. Kallel, L. Millet, A. Stock, J. L. Turon, and S. Wirth. 2013. North–south palaeohydrological contrasts in the central Mediterranean during the Holocene: tentative synthesis and working hypotheses. *Climate of the Past* 9 (5):2043-2071.

50 Marriner, N., C. Flaux, D. Kaniewski, C. Morhange, G. Leduc, V. Moron, Z. Chen, F. Gasse, J.-Y. Empereur, and J.-D. Stanley. 2012. ITCZ and ENSO-like pacing of Nile delta hydro-geomorphology during the Holocene. *Quaternary Science Reviews* 45:73-84.

51 Marriner, N., C. Flaux, C. Morhange, and J.-D. Stanley. 2013. Tracking Nile Delta Vulnerability to Holocene Change. *PLOS ONE* 8 (7):e69195.

52 Marriner, N., C. Morhange, and J. p. Goiran. 2010. Coastal and ancient harbour geoarchaeology. *Geology Today* 26 (1):21-27.

53 Meinardus, O. F. A. 1992. *Monks and Monasteries of the Egyptian Deserts* Revised Edition. Cairo: The American University in Cairo Press.

54 Nenna, M.-D. 2007. Production et commerce du verre à l'époque impériale : nouvelles découvertes et problématiques. *Facta : a Journal of Roman Material Culture Studies* 1:1000-1023.

55 Nenna, M.-D. 2010. Ateliers primaires de l'Égypte gréco-romaine : le site de Beni Salama dans le Wadi Natrun. *Archéopages. Archéologie et société* (Hors-série 2):122-127.

56 Nenna, M.-D., M. Picon, V. Thirion-Merle, and M. Vichy. 2005. Ateliers primaires du Wadi Natrum : nouvelles découvertes. In *Annales du 16e congrès de l'Association internationale pour l'histoire du verre, Londres, 2003*, 59-63.

57 Odum, W. E. 1988. Comparative Ecology of Tidal Freshwater and Salt Marshes. *Annual Review of Ecology and Systematics* 19 (1):147-176.

58 Pansu, M., and J. Gautheyrou. 2006. *Handbook of Soil Analysis*. Berlin, Heidelberg: Springer.

59 Park, L. E., K. Martens, and A. S. Cohen. 2002. Phylogenetic Relationships of Gomphocythere (Ostracoda) in Lake Tanganyika, East Africa. *Journal of Crustacean Biology* 22 (1):15-27.

60 Reimer, P. J., W. E. N. Austin, E. Bard, A. Bayliss, P. G. Blackwell, C. B. Ramsey, M. Butzin, H. Cheng, R. L. Edwards, M. Friedrich, P. M. Grootes, T. P. Guilderson, I. Hajdas, T. J. Heaton, A. G. Hogg, K. A. Hughen, B. Kromer, S. W. Manning, R. Muscheler, J. G. Palmer, C. Pearson, J. van der Plicht, R. W. Reimer, D. A. Richards, E. M. Scott, J. R. Southon, C. S. M. Turney, L. Wacker, F. Adolphi, U. Büntgen, M. Capano, S. M. Fahrni, A. Fogtmann-Schulz, R. Friedrich, P. Köhler, S. Kudsk, F. Miyake, J. Olsen, F. Reinig, M. Sakamoto, A. Sookdeo, and S. Talamo. 2020. The IntCal20 Northern Hemisphere Radiocarbon Age Calibration Curve (0–55 cal kBP). *Radiocarbon* 62 (4):725-757.

61 Ruiz, F., M. Abad, A. M. Bodergat, P. Carbonel, J. Rodríguez-Lázaro, M. L. González-Regalado, A. Toscano, E. X. García, and J. Prenda. 2013. Freshwater ostracods as environmental tracers. *International Journal of Environmental Science and Technology* 10 (5):1115–1128.

62 Topographic map. 1926. Called "Wadi El Natrun". Scale 1:100000. Sheet: 84/54, Produced by the Survey of Egypt, 25/690/3, Cairo.

63 Walter, E., and J. R. Dean. 1974. Determination of Carbonate and Organic Matter in Calcareous Sediments and Sedimentary Rocks by Loss on Ignition: Comparison with Other Methods. *Journal of Sedimentary Petrology* 44 (1):242-248.

64 Youssef, T., M. I. Gad, and M. M. Ali. 2012. Assessment of Groundwater Resources Management in Wadi El-Farigh Area Using MODFLOW. *IOSR Journal of Engineering* 2 (10):69-78.

List of illustrations

Title	**Fig. 1**
Caption	(A) The general location of the study area. (B) The site of *Bani Salama* in the *Wadi El-Natrun* depression. (C) Details of the *Bani Salama* site.
URL	http://journals.openedition.org/mediterranee/docannexe/image/14405/img-1.jpeg
File	image/jpeg, 609k

Title	**Fig. 2. Natural context of *Bani Salama***
Caption	This figure shows the geological, geomorphological and hydrological characteristics of the study area. It was drawn using a (Geological map 1987) produced by the Egyptian general petroleum corporation and CONOCO Coral Company, scale 1: 500,000. The digital elevation model (DEM) has a spatial resolution of 30 m and was produced using data from the Shuttle Radar Topography Mission (SRTM), NASA. The feature classes were drawn, and the contour lines were extracted from the DEM using ArcGIS 10.1.
URL	http://journals.openedition.org/mediterranee/docannexe/image/14405/img-2.jpeg
File	image/jpeg, 233k

Title	**Fig. 3.**
Caption	(A) The blocks of the Pharaonic temple gate from the 12th Dynasty. (B) The black granite bust from the 18th Dynasty of the Pharaonic period. (C) Beni Salama workshop was used to produce raw glass during the Roman period.
Credits	The photos A & C were taken during field study in June 2015 by Clément Flaux. Photo B was taken from (Fakhry 1942) and is an artefact found at *Bani Salama*.
URL	http://journals.openedition.org/mediterranee/docannexe/image/14405/img-3.jpeg
File	image/jpeg, 621k

Title	**Fig. 4.**
Caption	The ancient desert route connecting *Wadi El-Natrun* depression with El-Tarrana city
Credits	This figure was drawn using the topographic map of *Wadi El-Natrun* depression produced in 1926 by the Egyptian Survey Authority (Scale 1:100000). The ancient desert route that connected *Wadi El-Natrun* depression with El-Tarrana city was digitized in ArcGIS 10.1. This ancient desert route is not straight but varies according to the topography. El-Tarrana port served as a point of export for raw glass from *Wadi El-Natrun* during the Roman period.
URL	http://journals.openedition.org/mediterranee/docannexe/image/14405/img-4.jpeg
File	image/jpeg, 143k

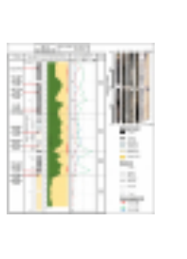

Title	**Fig. 5. The sediment core from *Bani Salama***
Caption	The core was extracted during a field study in June 2015 and the figure was drawn using Inkscape v. 0.91.
URL	http://journals.openedition.org/mediterranee/docannexe/image/14405/img-5.jpeg
File	image/jpeg, 566k

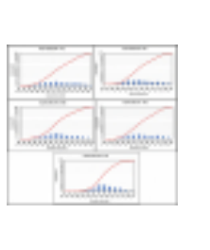

Title	**Fig. 6. Results of grain size analysis of sands taken from unit A.**
Caption	The figure shows the distribution of sand grain-size classes in five samples of core NAT-11. This analysis was carried out at the CEREGE laboratory in France by the authors and the results were processed using Excel.
URL	http://journals.openedition.org/mediterranee/docannexe/image/14405/img-6.jpeg
File	image/jpeg, 349k

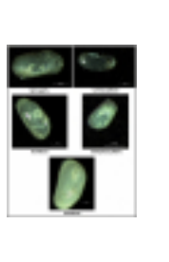

Title	**Fig. 7. The main species of Ostracod in the *Bani Salama* core**
Caption	Ostracod species include (*Candona* sp., *Gomphocythere* sp., *Limnocythere* sp., *Heterocypris* sp. and *Ilyocypris* sp.). This analysis was carried out by the authors at the Chrono-Environment Laboratory in Besançon, France.
URL	http://journals.openedition.org/mediterranee/docannexe/image/14405/img-7.jpeg
File	image/jpeg, 369k

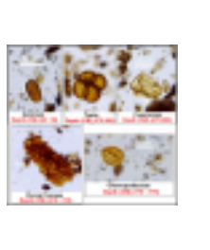

Title	**Fig. 8. The main pollen grains in the *Bani Salama* core.**
Caption	The figure shows some pollen types from the *Bani Salama* core (Typha, Apiaceae, Chenopodiaceae, Cyperaceae and Poaceae). This analysis was carried out by the authors at the Chrono-Environment Laboratory in Besançon, France.
URL	http://journals.openedition.org/mediterranee/docannexe/image/14405/img-8.jpeg
File	image/jpeg, 552k

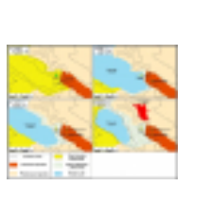

Title	**Fig. 9. Reconstruction of the Holocene paleogeography of *Bani Salama***
Caption	This figure shows the evolving geomorphology of the study area during four different stages, from around 6600 cal. BC to the present
Credits	The maps were drawn using ArcGIS, based on the core data from our study, maps and the digital elevation model (DEM).
URL	http://journals.openedition.org/mediterranee/docannexe/image/14405/img-9.jpeg
File	image/jpeg, 566k

Title	**Fig. 10. Tentative reconstruction of *Fasda* Lake levels during the past 8000 years and comparison with other regional proxies**
Caption	Holocene insolation at 30°N for June-July-August (Laskar *et al.*, 2004). (B) On the right axis: radiocarbon dates from early and mid-Holocene occupation sites in the Eastern Sahara (Kuper and Kröpelin, 2006). The solid black line denotes a three-point moving average. On the left axis: estimates for the population of the Nile valley in Egypt (Butzer, 1976). (C) North African lake levels (Magny *et al.*, 2013). (D) Reconstruction of *Fasda* Lake levels from core Nat-11 (this study). (E) Strontium isotope record from Mayut Lake on the western margin of the Nile Delta showing variations in the influence of the Mediterranean Sea and Nile flow in the lake's palaeohydrology (Flaux *et al.*, 2013). (F) Nile Delta accretionary status (Marriner *et al.*, 2013).
URL	http://journals.openedition.org/mediterranee/docannexe/image/14405/img-10.jpg
File	image/jpeg, 165k

References

Electronic reference
Gamal Younes, Clément Flaux, Isabelle Jouffroy-Bapicot and Nick Marriner, "Reconstruction of the Holocene Paleogeography of *Bani Salama*, *Wadi El-Natrun*, Egypt", *Méditerranée* [Online], Paleoenvironment, Geoarchaeology, Historical Geography, Online since 24 March 2023, connection on 27 March 2023. URL: http://journals.openedition.org/mediterranee/14405

About the authors

Gamal Younes
Aix-Marseille Université, CNRS, IRD, INRAE, CEREGE, Aix-en-Provence, France ; Department of Geography and GIS, Faculty of Arts, Ain Shams University, Cairo, Egypt, Younes@Cerege.fr, https://orcid.org/0000-0002-2270-5357

Clément Flaux
Mosaïques Archéologie, domaine la Barthe, 34660 Cournonterral, France, flaux.clement@gmail.com

By this author

À quand remonte l'état de référence « naturel » du Vistre de la Fontaine (Nîmes) ? [Full text]
At which time the Vistre de la Fontaine river (Nîmes, France) was natural ?
Published in *Méditerranée*, Paleoenvironment, Geoarchaeology, Historical Geography

Géoarchéologie de Port-la-Nautique (étangs narbonnais) [Full text]
Published in *Méditerranée*, Paleoenvironment, Geoarchaeology, Historical Geography

An Early Bronze Age pile-dwelling settlement of discovered in Alepu lagoon (municipality of Sozopol, department of Burgas), Bulgaria [Full text]
Découverte d'un site palafitte de l'âge du bronze ancien dans la lagune d'Alepou (municipalité de Sozopol, département de Burgas), Bulgarie
Published in *Méditerranée*, 126 | 2016

Connexion de la région lagunaire d'Alexandrie au Nil depuis 2 000 ans : entre contrôle anthropique et forçage naturel [Full text]
Alexandria's lagoonal hinterland and its connection to the Nile since 2000 BP: human impacts and natural forcing agents
Published in *Méditerranée*, 117 | 2011

Isabelle Jouffroy-Bapicot
LCE, Laboratoire Chrono-environnement, Université de Franche-Comté, France, Isabelle.jouffroy@univ-fcomte.fr, https://orcid.org/0000-0001-5920-7565

Nick Marriner
CNRS, ThéMA, Université de Franche-Comté, UMR 6049, MSHE Ledoux, 32 rue Mégevand, 25030 Besançon Cedex, France , Nick.marriner@gmail.com, https://orcid.org/0000-0002-7916-6059

By this author

Emergence of agriculture on the Taman Peninsula, Russia [Full text]
Émergence de l'agriculture dans la péninsule de Taman, Russie
Published in *Méditerranée*, 126 | 2016

Introduction [Full text]
Foreword [Full text | translation | en]
Published in *Méditerranée*, 122 | 2014

Caspian Sea-level changes at the end of Little Ice Age and its impacts on the avulsion of the Gorgan River : a multidisciplinary case study from the southeastern flank of the Caspian Sea [Full text]
Changements du niveau relatif de la mer Caspienne pendant le petit âge de glace et impacts sur l'avulsion du Gorgan
Published in *Méditerranée*, 122 | 2014

Évolution géomorphologique de la façade maritime d'Alexandrie (Égypte) au cours des six derniers millénaires [Full text]
Geomorphological evolution of Alexandria's maritime façade during the past 6000 years
Published in *Méditerranée*, 104 | 2005

Fire in Mediterranean Ecosystems: ecology, evolution and management [Full text]
J.E. KEELEY, W.J. BOND, R.A. BRADSTOCK, J.G. PAUSAS, P.W. RUNDEL, (2012), Cambridge University Press, 515 p.
Published in *Méditerranée*, 121 | 2013

Géoarchéologie en Méditerranée [Full text]
Programmes ArchéoMed-PaléoMed
Published in *Méditerranée*, 117 | 2011

All documents

Copyright

All rights reserved